# CHAPTER 5

# POTENTIAL ALTERNATIVES TO CURRENT CHOLINESTERASE INHIBITORS: AN *IN-SILICO* DRUG REPURPOSING APPROACH*

**Abstract**

Acetylcholinesterase/Butyrylcholinesterase inhibitors are considered an effective method for treating Alzheimer's disease (AD). With this disease's increasing prevalence and overall global burden, treatment options need to be increased in the next few years. Research on small molecule approval takes a longer time. Drug repurposing is a well-sought-out strategy to escalate the process of novel drug discovery. In this work, we have computationally analysed 11 new small molecule drugs used in various neurological diseases and Donepezil, a known acetylcholinesterase inhibitor, as a positive control. We investigated these drugs for possible fundamental interactions with acetylcholinesterase and butyrylcholinesterase, as both are critical in the pathophysiology of Alzheimer's disease. We have selected FDA-approved compounds for repurposing as possible inhibitors of these enzymes and novel therapeutic options for Alzheimer's disease. We selected the top two drugs for each protein for their binding energies and interactions based on their molecular docking analysis and Donepezil, the most commonly used drug for AD treatment. Molecular simulation and dynamics studies of the top 2 drugs in each case and free energy analysis helped us reach further conclusions about the best possible drugs for repurposing. Brexipirazole and Deutetrabenazine produce encouraging results as butyrylcholinesterase and acetylcholinesterase inhibitors, respectively.

---

* Part of the work is published in Kundu D, Dubey VK (2021) Potential alternatives to current cholinesterase inhibitors: an *in-silico* drug repurposing approach. Drug Dev Ind Pharm. 47, 919-930.

**5.1 Introduction:**

Neurodegenerative diseases, specifically the class coming under protein misfolding diseases, are among the recent and most formidable medical science challenges. Among these neurodegenerative diseases, Alzheimer's disease has the most significant impact worldwide, with as many as 46.8 million people being affected annually. Further, it is also projected that there will be three-fold higher AD cases by the year 2050 (Martin *et al.,* 2016, Lopes *et al.,* 2018, Kundu *et al.,* 2020, Kundu *et al.,* 2020). The significant hypotheses that are now widely accepted regarding Alzheimer's include the amyloid cascade hypothesis, metal stress hypothesis, oxidative stress hypothesis, tau hyperphosphorylation, and cholinergic hypothesis (Larik *et al.*, 2017; Lv *et al.*, 2017, Lopes *et al.,* 2018, Kundu *et al.* 2020). The cholinergic hypothesis is most accepted and highly targeted toward drug development. The cholinergic hypothesis clearly states that the increased activity of acetylcholinesterase in early stages and butyrylcholinesterase in later stages are the main culprit. Their activity results in an excess breakdown of acetylcholine's critical neurotransmitter into its components, thus disrupting standard neuronal transmission. Drugs that could specifically inhibit their activity could help treat the pathological condition. Increasing the amount of acetylcholine in synaptic clefts and prolonging their activity would ultimately lead to improved conditions preventing the accelerated loss in cognition (Tai *et al*., 2003; Bartus, 2000, Lopes *et al.,* 2018).

Additionally, the already marketed and prescribed drugs have raised concerns about their long-term efficacy, which enhances the need to search for other potential drugs with a similar mechanism that might prove to have more effects in the long term (Tore *et al*., 2012, Ujan *et al*., 2019). The current commercially available drugs forming the front line against advanced AD stages, including Rivastigmine, Neostigmine, Physostigmine, Donepezil and Memantine, have other physiological consequences for the consumer. Reports of side effects include problems associated with gastrointestinal disturbances, vomiting, heartburn, diarrhoea, loss of appetite, headache, and hepatotoxicity. As a result, drug development in this area of medical science has always been challenging. In the last decade or so, only 25 drugs have been passed to Phase II/ Phase III clinical

trials for AD, whereas the number of drugs in the same time and the same stage for cancer is as high as 1600-1700 (Kim, 2015, Shaik *et al.* 2010, Kumar *et al.* 2017). These are real issues in drug development; scientists have long been engaged in effective drug repurposing for this matter. Drug repurposing, at its core, can be a very effective method of discovering multiple uses of a standard drug that has already been approved by the FDA and is currently in use. One of the most significant advantages of taking up this process is reducing a novel drug's production cost from scratch. Repurposing does save not only money but also time and other industrial resources.

Some of the recent notable work done previously by various groups have focused on the usage of Non-steroidal anti-inflammatory drugs (NSAIDs) in neurodegenerative diseases (Terzi *et al.* 2017), use of 1, 3, 4- Thiadiazole conjugates as mixed inhibitors against AChE (Ujan *et al.* 2019), a study on 1-acetyl 3-aryl thiourea derivatives using both molecular docking and enzymatic assay (Saeed *et al.* 2017) and simple repurposing of antipsychotic drugs as anti-Alzheimer's disease agents (Kumar *et al.* 2017). The current computational study aims at molecular docking, molecular dynamics, and simulation studies with subsequent analysis of recently approved small molecule drugs for other neuro-psychological diseases from 2015-2020. Using extensive computational approaches, the current study is crucial to understanding the dynamics of any reversible inhibitor against these enzymes. We performed molecular docking in the reported catalytic sites of Acetylcholinesterase and Butyrylcholinesterase as potentially reversible inhibitors of these enzymes. The details of the drugs based on their usage, and year of approval, are provided in Table 5.1. Further, we have tried to conclude the most significant potential inhibitor for butyrylcholinesterase and acetylcholinesterase through molecular simulation and dynamics studies. We have used standard GROMACS analytical tools to analyse and interpret the simulation results.

**Table 1.1-** Small molecule drugs used in the current study, their usage and year of approval by the FDA

| S No | Drug Approved | Original Use | Year of Approval |
|---|---|---|---|
| 1. | Opicapone | Parkinson's experiencing off episodes | 2020 |
| 2. | Istradefylline | Parkinson's experiencing off episodes | 2019 |
| 3. | Ozanimod | Multiple sclerosis | 2020 |
| 4. | Siponimod | Multiple Sclerosis | 2019 |
| 5. | Tafamidis megulmine | ATTR | 2019 |
| 6. | Safinamide | Parkinson's Disease | 2017 |
| 7. | Pimavanserin | Treatment of Hallucinations and Delusions in PD | 2016 |
| 8. | Leumateperone tosylate | Schizophrenia | 2019 |
| 9. | Cariprazine | Schizophrenia & BPD | 2015 |
| 10. | Brexipiperazole | BPD & Major Depressive disorder | 2015 |
| 11. | Donepezil | Treatment of AD, an acetylcholinesterase inhibitor | 1996 |
| 12. | Galanthamine | Treatment of AD, an acetylcholinesterase inhibitor | 2001 |
| 13. | Rivastigmine | Treatment of AD, an acetylcholinesterase inhibitor | 2000 |
| 14. | Deutetrabenazine | Treat chorea for Huntington's disease | 2019 |

Acetylcholinesterase (AChE: 3.1.1.7) is found in various conducting tissues such as nerves and muscles, central and peripheral tissues, motor and sensory fibres and cholinergic and non-cholinergic fibres. They are more prominent in motor neurons than in sensory neurons. The enzyme has various molecular forms of existence, having similar catalytic properties and differences in their arrangement and mode of attachment to the cell surface. The main form of acetylcholinesterase enzyme in the mammalian brain is the tetrameric form G4 (Wang and Tang, 2005). Acetylcholine is the primary substrate and the most crucial neurotransmitter on which acetylcholinesterase works. The neurotransmitter was first described in autonomic ganglia, neuromuscular junctions, and many synapses in the central nervous system. It is also the primary neurotransmitter in the preganglionic sympathetic and parasympathetic neurons and the adrenal medulla. Acetylcholine is mainly found in interneurons and some long axon cholinergic pathways in the central nervous system. One of the essential pathways of degeneration associated with AD's pathophysiology is the cholinergic projection from the *nucleus basalis* of Meynert in the basal forebrain to the forebrain neocortex and

associated limbic structures (Perry *et al.,* 1999, Colovic *et al.,* 2013). Acetylcholinesterase is majorly involved in terminating the impulse transmission by hydrolysing acetylcholine into choline and acetic acid in various pathways in the central and peripheral nervous system. The enzyme's inactivation by various inhibitors mainly focuses on the accumulation of acetylcholine, overstimulation of muscarinic receptors, and disrupted neurotransmission. It is one of the primary reasons acetylcholinesterase inhibitors are important as drug targets in various diseases.

Butyrylcholinesterases (BuChE: 3.1.1.8) is another serine hydrolase enzyme responsible for hydrolysing AChE, especially in the later stages of AD. Acetylcholinesterase is known to be more active during the early phases of neurodegeneration. In advanced stages, its activity decreases, and the activity of butyrylcholinesterase increases. One of the significant goals of drug development in this context is mainly targeted toward inhibitory activity towards acetylcholinesterase and butyrylcholinesterase (Bono *et al.,* 2015, Li *et al.,* 2017, Lopes *et al.,* 2018).

### 5.2 Methodology

**5.2.1 Protein Preparation:** Based on the selection of wild-type human Acetylcholinesterase (PDB ID: 4EY7) and human Butyrylcholinesterase (PDB ID: 4BDS) structures were selected on the resolution for each of them. Also, we wanted to choose a protein for our docking with no mutation. We selected PDB structures and the FASTA sequence from the RCSB PDB site URL rcsb.org (Berman *et al.* 2000). We further used PyMol visualising tool to remove water molecules and other heteroatoms or ligands, which were complex with the protein (De Lano, 2002; MacDonald *et al.,* 2012). The energy minimisation of the protein was performed using SWISS PDB Viewer as described in our previous study (Umesh *et al.,* 2020, Guex and Peitsch, 1997). We performed pre-processing of protein structures, including the addition of Gasteiger charges and hydrogen addition, which were done using Chimera 1.13 (Pettersen *et al.* 2004) as described in previous literature (Butt *et al.* 2019).

**5.2.2 Target Site Identification for Molecular Docking:** The target site was selected based on available literature on catalytically active regions of the enzymes from a recent study (Lopes *et al.*, 2018).

*Homo sapiens* Acetylcholinesterase (HsAChE) belongs to the serine hydrolases class, mainly found in the brain's neuromuscular junctions and synapses. It is known to have a very high and significant catalytic activity, with each molecule of acetylcholinesterase degrading about 25,000 molecules of acetylcholine per second (Taylor and Radic, 1994, Colovic *et al.,* 2013). Structurally the enzyme monomer is α/β protein containing 12 stranded central mixed β sheet containing 14α helices. The enzyme's active site is close to the molecule base and contains two subsites, the anionic subsite, the catalytic centre (CAS), and the esteratic subsite, which is the choline-binding pocket. All the 14 amino acid residues that form the aromatic gorge in acetylcholinesterase are highly conserved among various species. One of the critical amino acids in this gorge is Tryptophan84, whose deletion reduces the enzyme activity by almost 3000 times (Tougu *et al.* 2001, Colovic *et al.* 2013). This tryptophan residue is also known to help acetylcholine bind at the esteratic subsite, which contains a catalytic triad similar to all other serine hydrolases: Ser200, His440, and Glu327 via interactions with quaternary nitrogen of acetylcholine (Lopes *et al.*2018). There are also specific amino acids adjacent to the CAS containing Phe288, Phe290 and Phe331 (Acyl pocket) and Gly118, Gly119 and Ala201 (Oxyanion hole). These two sites mainly function to prevent hydrolysis of heavy esters by selectively binding with them and forming a significant portion of the active site gorge. In addition to these two subsites, the enzyme contains peripheral anionic sites other than the active site's choline-binding pocket. These sites bind acetylcholine and other quaternary ligands and are involved in substrate-based inhibition (Lopes *et al.*, 2018). The Peripheral binding sites in human AChE contain essential residues like Asp74 and another aromatic amino acid, Trp286, implicated in modulating the central catalytic triad activity below (MacDonald *et al.* 2012).

A high level of structural homology is shared between Hsacetylcholinesterase and *Homo sapiens* butyrylcholinesterase (Hsbutyrylcholinesterase) with almost 65% homology and sharing similar residues in the active site: Ser198, His438 and Glu325. One of the significant differences between AChE and BuChE is the absence of bulky aromatic amino acids in the acyl pocket of BuChE (Saxena *et al.,* 1997, Lopes *et al.,* 2018). We have listed the detailed coordinates of the various grid parameter files of these proteins in Table 5.2.

**Table 5.2-** Details of the proteins used for docking, the sites of docking and their respective coordinates and references

| Protein | Grid Box | Docking Site | Coordinates (X, Y, Z) | Reference (Docking Site) |
|---|---|---|---|---|
| *Hs*AChE | 1 | Asp73, Trp285, Tyr 71 (PAS), Tyr123 Trp85 (Choline Binding Site) Glu333, His446, Ser202 (Catalytic Triad), Tyr336, 340, Phe337, | -11.436, -41.035, 30.309 | MacDonald *et al*. 2012 Colovic *et al.* 2013 |
| *Hs*BuchE | 1 | Asn67, Asp70, Trp82, Gln119, Tyr332, Phe329, Ala328 (PAS), Ser198, Glu325, His438 (Catalytic Triad), Ala277 | 17.067,42.234,37.023 | MacDonald *et al.* 2012 |

**5.2.3 Selection and Preparation of Ligands:** The list of compounds used in the current study is shown in Table 5.1. A total of 11 small molecule drugs that the FDA has recently approved for various other neurological and neurodegenerative conditions have been used, along with three already approved and used acetylcholinesterase inhibitor positive controls. We used the PubChem and Drugbank databases to avail the 3D structure of the ligands in the sdf format as previously reported (Umesh *et al.* 2020, Kundu *et al.* 2020). The structures were subject to dock prep using Chimera 1.13 (Pettersen *et al.* 2004). We further prepared ligands, including energy minimisation, removal of solvents and setting of rotatable bonds and torsion of ligands as described previously (Kundu *et al*., 2020, Umesh *et al.,* 2020).

**5.2.4 Compound Screening and Molecular Docking:** Molecular screening of all the ligands was carried out using Raccoon and MGLTools v. 1.5.6 by AutoDock as the docking engine (Morris *et al.,* 2009, Umesh *et al.,* 2020). The ligands were kept flexible for the molecular docking process, and the protein as a rigid structure. We generated the configuration files for the various proteins and the respective grid box coordinates, generating docking parameter files and grid parameter files using integrated AutoDock and AutoGrid tools of the AutoDock4 platform (Umesh *et al.,* 2020). The grid boxes were selected to cover a portion of the selected amino acids, one site at a time.

The primary docking protocol we followed used the standard Lamarckian Genetic Algorithm (LGA) using AUTODOCK4 (Morris and Olson, 1996; Umesh *et al.,* 2020, Kundu *et al.,* 2020). LGA is much better than other simulated or search algorithms available within the AUTODOCK platform. The algorithm uses the AMBER force field based on the previous five terms described in the literature (Venkatesan *et al.,* 2010, Kundu *et al.,* 2020). We generated docking parameter files of each ligand, mainly using the initial population's default settings and the total number of evaluations described previously in our works. We used the AUTODOCK4 platform for validation and analyses of the various docked conformations, and we studied conformation with the lowest binding energy for various interactions (Venkatesan *et al.,* 2010, Umesh *et al.,* 2020, Kundu *et al.,* 2020).

### 5.2.5 Molecular Dynamic Simulation Studies:

We performed molecular dynamics and simulation studies to validate our docking results using apoprotein and protein-ligand complexes. We simulated the top two drugs along with Donepezil as a positive control. For our simulation studies, we used GROMACS v 2018.8. PRODRG server v. 2.5 (van Aalten *et al.* 1996, Borkotoky and Banerjee, 2020) was used to generate the topological and parameter files for our ligands using the GROMOS force field. For pre-processing of the apoprotein and the ligand complexes, we also used the GROMOS 54a7 force field and used SPC/E water molecules (Abraham *et al.* 2015) for the solvation of the system in a cubic box of 1.2 nm.

Further, we used Na+ and Cl- ions as required to neutralise the charge of the systems in the ionisation step. We used the steepest descent algorithm for the energy minimisation step for all systems with a 1000 kJ/mol tolerance. We set the maximum number of steps for energy minimisation at 50,000. The cut-off value set for both long-range and short-range interactions was 1.2 nm, using the PME method. Post energy minimisation, we carried out NVT and NPT equilibration steps for 1ns with a fixed number of particles, volume and temperature. We performed NVT equilibration using the Berendsen thermostat (Bussi *et al*., 2007, Borkotoky and Banerjee, 2020) with velocity rescaling at a temperature of 300K with a time step of 0.1 ps. We used Particle Mesh Ewald (PME) (Kawata and Nagashima, 2001) method for long-range interactions cut-off value was set at 1.2 nm and a Fourier spacing of 0.16 nm. For NPT equilibration, we used a fixed number of particles, pressure and temperature. We initiated Berendsen isotropic pressure coupling with a time constant of 2 ps, a reference bar of 1.0 atm and isothermal compressibility of a $4.5e^{-5}$ bar. After completing both the equilibration steps, we simulated all the systems for 100 ns with a dt of 2 fs and a leap-frog integrator (Borkotoky and Banerjee, 2020). We analysed the simulation results using standard commands used for GROMACS platforms. We used the LINCS algorithm to strain all the bond lengths (Hess *et al.* 1997).

**5.2.6-MM/PBSA Free Energy Analysis:** We used the MM/PBSA tool for analysing the binding mode and total free binding energy for our top two ligands and Donepezil with our enzymes. We used the package within the GROMACS working environment using the gmx_mmpbsa tool and pbsa.mdp script. We performed the free energy analysis for the last 20ns of the run to reduce computational time. The solute and the solvent dielectric constants were 2 and 80, respectively (Kar *et al.*, 2013, Genheden and Ryde, 2015, Musyoka *et al.*, 2016, Gupta and Dasmahapatra, 2020).

5.2.7-Visual analysis**:** We selected the lowest conformation for each ligand in the various proteins. Analysis of interactions, numbers and types were done in PyMol- 2.3.0 (DeLano, 2000) and Discovery Studio Visualizer to generate 2D diagrams depicting the various interactions (Discovery Studio, Dassault Systemes, BIOVIA, San Diego, CA, USA, 2020). The interactions were also

validated using Protein-Ligand Interaction Profiler (PLIP) (Salentin *et al.* 2015), and LigPlot+ were also used to generate 2D diagrams (Lawonosky *et al.* 2011).

**5.2.8-ADME and Toxicity analyses:** Although the FDA has previously approved all the drugs, we still ran the drugs for a customary ADMET analysis using the SWISS ADME software (Diana *et al.* 2017) and were noted for any violations of Lipinski's rule (Kundu *et al.* 2020). We have represented the results of the ADME analysis in Table 5.7.

**5.3-Results:** The details of the interaction patterns of various proteins used in this study, along with their respective inhibitor constants, we represented the two best drugs from each set of molecular docking in Table 5.3 and Table 5.4.

**5.3.1-Docking results with Acetylcholinesterase of Homo sapiens:**

As mentioned earlier, the active site of the human acetylcholinesterase contains the catalytic triad (Ser202, His446 and Glu333), the acyl binding pocket containing Phe294 and 296, the oxyanion hole (Gly120, Gly121 and Ala203), and amino acid residues of the PAS (Tyr72, Asp74, Tyr286, 340). The grid box encompassed the majority of these amino acids. The top two molecules were Deutetrabenazine (-8.7 kcal/ mol) and Siponimod (-8.6 kcal/ mol). Among the positive controls, Donepezil showed a higher binding affinity (-8.5 kcal/mol). Deutetrabenazine showed a hydrogen bond with Tyr336, a vital amino acid residue in the PAS of the enzyme, and Pi-Pi stacking interaction with Trp123, Pi alkyl interaction with Tyr340 and Pi-Cation interaction with Trp285. We observed significant Van Der Waals interaction between the drug and the protein in the acyl pocket region and parts of the PAS. Involved amino acid residues were Leu288, Phe294, Arg295 from the acyl pocket and Tyr72 and Tyr340 from the PAS. On the other hand, Donepezil showed two hydrogen bond formations with Arg246. It was more heavily involved in van der Waals interactions with critical residues like Leu288, Ser292, Thr237, Val238, and Gln368. Pi-cation interaction with Arg295, Pi-alkyl and alkyl interactions with Pro289, Val299, Pro367, 234 (Figure 5.1A and 5.1B). Previous studies reported interactions with these residues by Kumar *et al.* 2017 where the authors subjected AChE to docking with various anti-psychotic drugs, among

which Donepezil and Pimozide showed the lowest energy and the best favourable interactions (Kumar *et al.* 2017). The interactions of the two drugs with acetylcholinesterase are represented in Fig 5.1. Recent studies, including computational data by Ujan *et al.* and Larik *et al.*, reported interactions with these critical residues (Ujan *et al*., 2019; Larik *et al*., 2017). The other ligands, especially Galanthamine (-7.3 kcal/mol) and Risvagtimine (-7.95 kcal/mol) showed lower binding energies than Donepezil and the chosen ligands. Some other ligands showed binding energy comparable to Donepezil, but some critical interactions were missing.

**Table 5.3-** Details of various ligand interactions, respective binding and intermolecular energy and inhibitor constant in Acetylcholinesterase from *Homo sapiens* (*Hs*AChE). Donepezil is the positive control which is already an approved acetylcholinesterase inhibitor by FDA.

| Ligand/Drug | Binding Energy (kcal/mol) | Hydrogen bonds | Non-Covalent Interactions | VDW Interactions | Hydrophobic interactions |
|---|---|---|---|---|---|
| Donepezil | -8.5 | Arg246 (2) | Arg295 (Pi-Cation), Pro289, Val299, Pro367, 234, 409 (Alkyl and Pi-Alkyl), Thr37 (C-H) | Leu288, Ser292, Val238, Trp235, Thr237, Val369, Leu539, Asn532, Cys408, Trp531, His404, Leu535, Pro536, Gln368 | Pro409, Trp531 (2), Leu539 |
| Deutetrabenazine | -8.7 | Tyr336 | Tyr123 (Pi-Pi Stacked), Phe296,337, Tyr340 (Pi-Alkyl), Ser292, Asp73 (C-H bond), Trp285 (Pi-Cation) | Tyr71, Leu288, Val293, Gly120, Phe294, Arg 295, Val293 | Trp285 (2), Phe296, Phe337, Tyr340 |
| Siponimod | -8.6 | N/A | Trp181, Pro51 (2), Leu177 (Pi-Alkyl and Alkyl), Glu184, Gln180 (Halogen, Fluorine) | Arg12, Asn185, Gly13, Trp55, Lys52, Phe36, Pro48, 49, Leu173, Arg176, Asp305 | Arg12, Pro48, 51 (2), Lys52, Leu173, 177 |

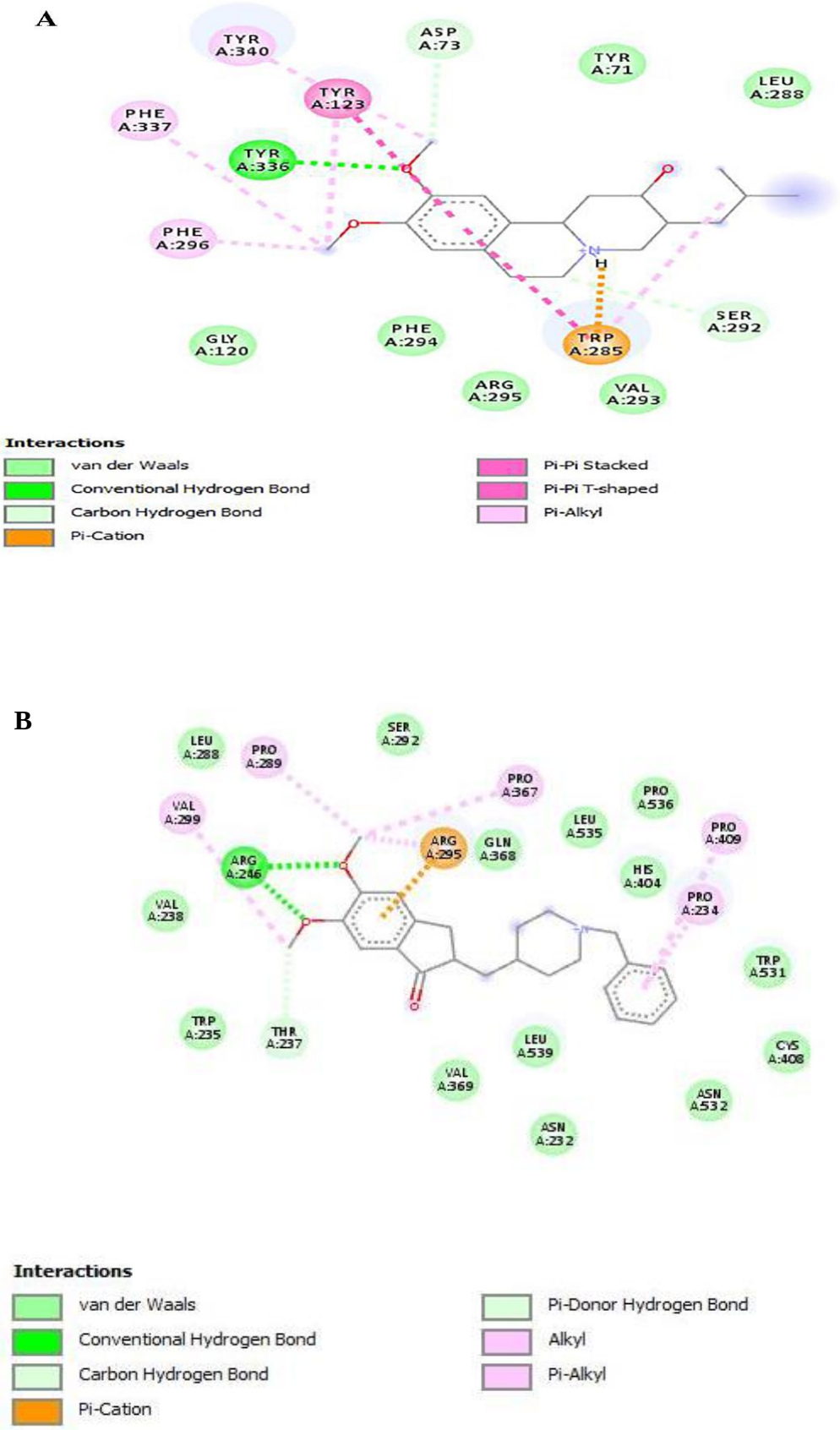


**Fig 5.1 Interaction of *Homo sapiens* Acetylcholinesterase (HuAChE): (A)** Deutetrabenazine and **(B)** Donepezil as seen in Discovery Studio Visualizer. Green dashed lines represent hydrogen bonding, Pink dashed lines represent Pi Alkyl and Pi T-shaped interactions, Purple dashed lines represent Pi- Sigma interactions, and the orange dashed lines represent attractive charges. The remaining interactions represent Van Der Waals interactions. Light Pink dashed lines represent C-H bond interactions.

### 5.3.2 Docking results with Butyrylcholinesterase of Homo sapiens:

It is crucial to carry out docking studies with acetylcholinesterase and butyrylcholinesterase as these enzymes show their respective activities on acetylcholine in different stages of the disease. As a result, drugs inhibiting Acetylcholinesterase and Butyrylcholinesterase can effectively treat AD. In this study, we report that Brexpiprazole (-10.81 kcal/mol), other than Pimavanserin (-10.23 kcal/mol) to show low binding energy and favourable interactions, although both were lower than Donepezil (-11.24 kcal/mol). Brexpiprazole also showed hydrogen bond interaction with Gly116. Trp82, His438, and Ala328 showed Pi sigma, Pi stacked, and Pi alkyl interactions, respectively, and are critical residues of PAS and the enzyme's active site. VDW interactions are shown by residues Ser198, Gly115, 117 and 121, Tyr128 and Phe329, whereas Trp82 shows hydrophobic interactions, Thr120, Phe329 and Tyr332. Pimavanserin formed hydrogen bonding with Gly116 and 117, both critical residues. It also showed various Pi interactions with critical aromatic amino acids like Tyr332, Phe329 and Trp82. Ser198, His438, Gly439, Pro285, Asn489 and Gly115, Phe318 show VDW interactions. Gly119, Phe329 and Tyr332 also show hydrophobic interactions. All the interactions are shown in Fig 2A and 2B. Kumar *et al.* 2017 reported similar interactions when they predicted Bromperidol to have AChE inhibitory activity. Galanthamine (-7.88 kcal/mol) and Risvagtimine (-6.99 kcal/mol) showed significantly lower binding affinity than Donepezil Brexipirazole or Pimavanserin (Fig 5.2 A-B).

The actual impact of the molecular docking depends on the ligands chosen and the protein of interest. Grid size, complex conformation and type of interactions play an essential role in the actual result of docking. Even if the binding energy is not very low, it does not necessarily imply the quality of docking to be weak; the actual interpretation in terms of types of interactions determines the stability of the protein-ligand conformation (Verma *et al.* 2016).

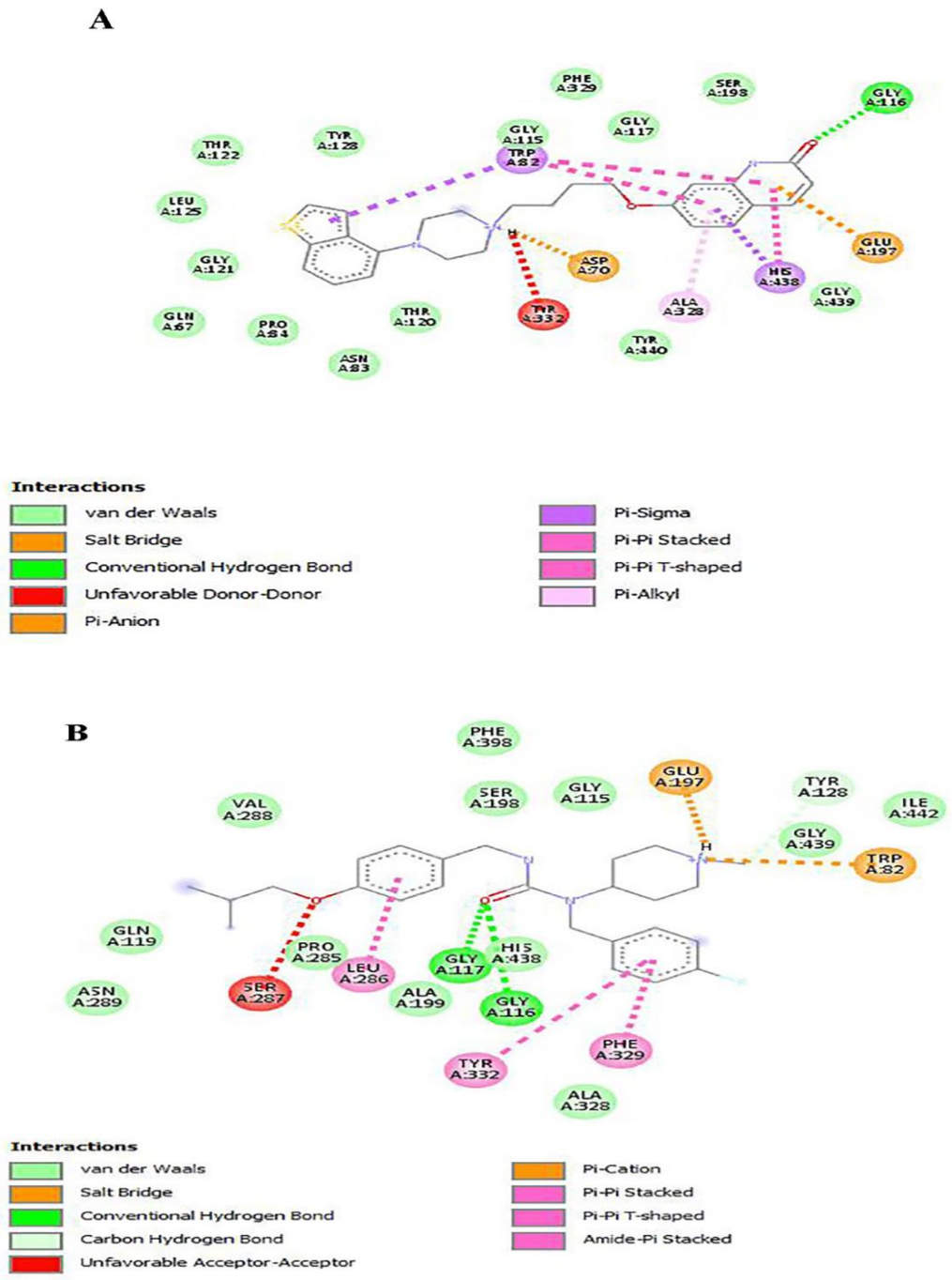


**Fig 5.2 Interaction of *Homo sapiens* Butyrylcholinesterase (HuBuchE) with**: **(A)** Brexipirazole and **(B)** Pimavansarin as seen in Discovery Studio Visualizer. Green dashed lines represent hydrogen bonding, Pink dashed lines represent Pi Alkyl and Pi T-shaped interactions, Purple dashed lines represent Pi- Sigma interactions, and the orange dashed lines represent attractive charges. The remaining interactions represent Van Der Waals interactions. Light Pink dashed lines represent C-H bond interactions.

**Table 5.4-** Details of various ligand interactions, respective binding and intermolecular energy and inhibitor constant in Butyrylcholinesterase from *Homo sapiens* (*Hs*BuChE). Donepezil is the positive control which is already an approved acetylcholinesterase inhibitor by FDA. VDW is Van Der Waal's interactions.

| Ligand/Drug | Binding Energy (kcal/mol) | Hydrogen bonds | Non-Covalent Interactions | VDW Interactions | Hydrophobic interactions |
|---|---|---|---|---|---|
| Donepezil | -11.24 | Pro285 | Trp231 (Pi Stacked), Leu286, Trp82, Pro284 (Alkyl & Pi-Alkyl) | Asn68, Ile69, Asn83, Asp70, Gly116,117, Tyr128, Ser198, Phe329 | Asp70, Trp231 (2), Leu286, Phe329, 398 |
| Brexipiprazole | -10.81 | Gly116 | Trp82 & His438 (Pi Sigma, Pi-Pi Stacked), Asp70 & Glu197 (Salt Bridge), Ala328 (Pi Alkyl) | Phe329, Gly115,117, 121, Ser198, Tyr128, Tyr440, Gly439 | Trp82 (3), Thr120, Phe329, Tyr332 |
| Pimavanserin | -10.23 | Gly116,117 | Leu286, Tyr332, Phe329 (Pi Stacked, Pi-T shaped and Pi- Amide interactions), Trp82 (Pi Cation), Glu197 (Salt Bridge) | Ser198, His438, Gly439, Ile442, Val288, Pro285, Asn289, Ala328, Gly115, Phe398 | Gln119 (2), Val288, Phe329, Tyr332 |

### 5.3.3 Molecular Simulation Results:

We performed five different analysis types on our simulated complexes to better understand the results. We used the gmx_rms tool to generate the RMSD trajectory of the apo and the holoprotein complexes, indicating the systems' overall stability. We also used the gmx_gyrate tool to determine the system's radius of gyration during the entire simulation period. We employed the gmx_rmsf tool to calculate the overall protein and complex rmsf(s). Further, we employed the gmx_hbond tool for calculating the average number of hydrogen bonds formed between the ligand and the protein, indicating a measure of the stability of the apoprotein and the favourable

interactions between the protein and ligand. The cut-off value between the donor and the acceptor atoms was set at 0.35nm.

**5.3.3.1 Simulation of Acetylcholinesterase:** We performed a similar simulation for acetylcholinesterase enzyme and Donepezil as the control and Deutetrabenazine and Siponimod as potential alternatives. The RMSD trajectory of all the three complexes compared to apoprotein yielded a result indicating both Siponimod and Deutetrabenazine had a better impact on the overall stability of the protein than Donepezil which had the highest RMSD deviation up to (0.34 nm). In contrast, the apoprotein and the complexes with Deutetrabenazine and Siponimod converged around 0.25 nm. The donepezil complex showed sudden fluctuation after 25 ns, and the RMSD was stable afterwards. The complex with Deutetrabenazine also showed minor fluctuations before 20ns, after which the RMSD trajectory remained stable throughout (Fig 5.3A). All three complexes show an increase in the overall protein's compactness in the radius of gyration trajectory (Rg) compared to the apoprotein, with Siponimod showing the highest compactness with a maximum deviation up to 2.3 nm. Both Donepezil and Deutetrabenazine showed a similar trajectory converging around 2.32 nm.

The apoprotein showed the maximum deviation with Rg trajectory, reaching up to 2.35 nm (Fig 5.3B). The RMSF graph also shows that the potential new drug molecules impact the complete protein better than Donepezil. As per our docking results, Siponimod interacts primarily with the N-terminal residues and few residues around the Ser203 position, impacting these regions the maximum and consequently reducing the RMSF values of amino acids stretch. Siponimod also shows the highest fluctuations in the C terminal residues between 500-540 amino acid stretch. Compared to Siponimod, Deutetrabenazine showed more consistency as it interacted with all the critical residues in the Peripheral anionic site and the catalytic triad. Hence, it significantly affects the RMSF of these residues, affecting the overall folding compactness of the protein. Donepezil showed similar fluctuation in the RMSF trajectories, interacting with similar residues during molecular docking. Deutetrabenazine and Donepezil also showed similar trajectories even in the

radius of gyration. The sudden fluctuation resulting in higher RMSF of residues around 350-400$^{th}$ amino acid stretch could be due to the sudden increase in the RMSD between 25-27$^{th}$ ns (Fig 5.3C). The hydrogen bond analysis showed that Donepezil and Siponimod had an average of less than one hydrogen bond over the entire simulation period.

**5.3.2.2 Simulation of Butyrylcholinesterase:** We performed a 50ns simulation of the butyrylcholinesterase apoprotein and the ligands. We used Donepezil as the positive control and compared our results with those generated from the novel ligands. The RMSD trajectories generated showed similar trajectories for the apoprotein and the complexes with Brexipiprazole and Pimavanserin. The three trajectories converged at around 0.22-0.25 nm (Fig 5.3A). RMSD trajectory of Donepezil continuously rose till 40ns compared to 10ns for the other systems. Further, it was stable throughout the simulation after 40ns. The results indicate better stability of the apoprotein in complex with the novel repurposed drugs. The radius of gyration trajectories indicating the overall compactness of the protein in the presence of the ligands showed almost similar overlapping trajectories for all the three complexes, Donepezil, Brexipiprazole and Pimavanserin.

Donepezil and Brexipiprazole converged around 2.3-2.31 nm, similar to the apoprotein (Fig 5.3D). The results indicate that both the novel repurposed drugs have a similar impact on the protein's compactness compared to the positive control. The RMSF result is encouraging as both complexes with the novel repurposed drugs Brexipiprazole and Pimavanserin showed much lower fluctuation than the apoprotein. The most significant impact on the fluctuation of residues was seen between the region 200-400$^{th}$ amino acid stretch, mainly containing the ligands' binding sites (Fig 5.3E). The hydrogen bond analysis showed an average formation of 1-2 hydrogen bonds over the entire simulation period for Brexipiprazole, less than one hydrogen bond for Donepezil and lesser average hydrogen bonds for Pimavanserin. Further, we performed the free energy analysis to understand which of the two novel repurposed drugs is a better potential candidate. We have provided the details of the energy analysis in Table 5.5. The overall binding free energy for

Brexipiprazole is -212.690 kcal/mol, and Pimavanserin is -108.626 kcal/mol, whereas Donepezil has overall binding energy of -180.517. All three values have Van Der Waal's force as the highest contributor in terms of energy. The results indicate that Brexipiprazole is a much better candidate than Pimavanserin. The significantly lower binding energy indicates that Brexipirazole binds to the protein's active site and other binding pockets with much higher affinity than Donepezil and Pimavanserin. The free energy analysis and the formation of hydrogen bonds align with each other, and so is the RMSD and the Rg trajectories.

**Table 5.5-** MM/PBSA free energy analysis of Donepezil, Brexipiprazole and Pimavanserin in complex with butyrylcholinesterase, SASA is Surface Accessible Surface Area.

| Ligand | Van Der Waals (kJ/mol) | Electrostatic (kJ/mol) | Polar Solvation (kJ/mol) | SASA (kJ/mol) | Binding Energy(kJ/mol) |
|---|---|---|---|---|---|
| Donepezil | -212.885±70.80 | -13.601±6.19 | 65.65±23.33 | -19.681±6.54 | -180.517±60.29 |
| Brexipiprazole | -252.648±10.60 | -10.394±3.981 | 71.703±9.437 | -21.351±0.948 | -212.69±13.772 |
| Pimavanserin | -131.238±86.14 | -9.815±9.36 | 45.382±32.44 | -12.955±7.92 | -108.626±70.323 |

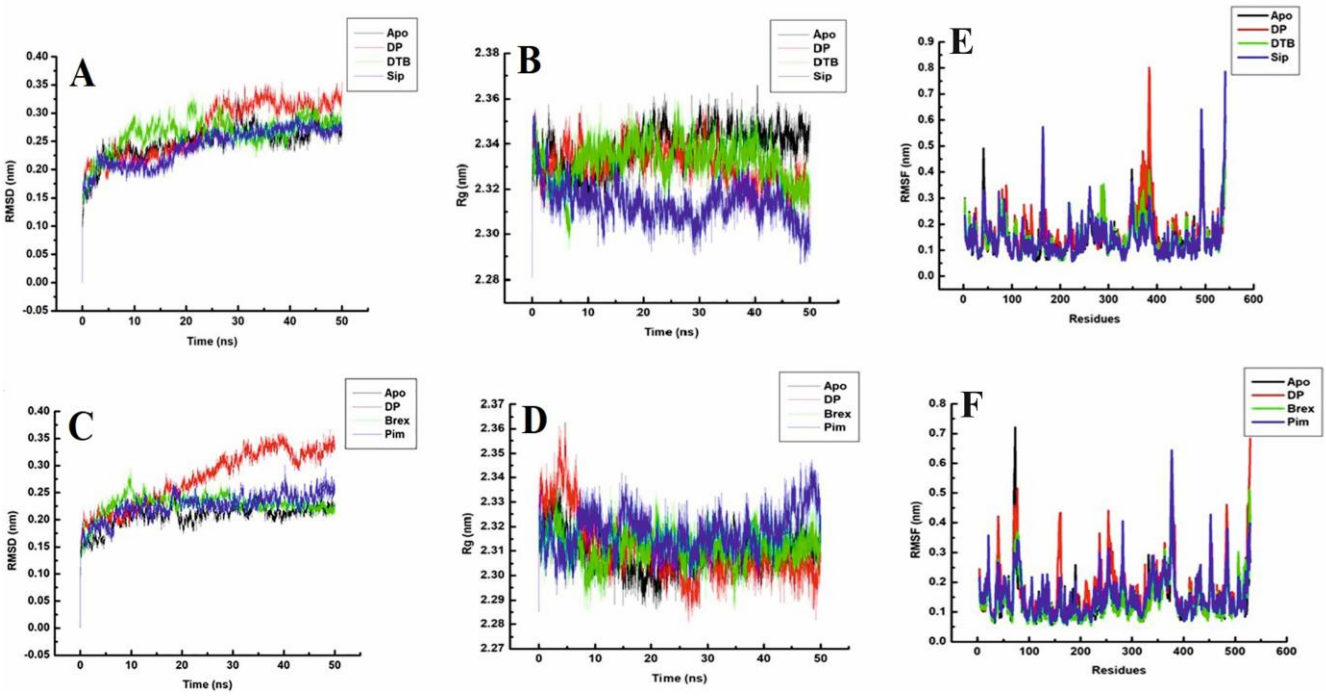

**Fig 5.3 Molecular Dynamics and Simulation of AChE and BuChE: (A)** RMSD and **(B)** Radius of Gyration of AChE **(C)** RMSD and **(D)** Radius of gyration of BuChE **(E)** RMSF of Acetylcholinesterase and **(F)** RMSF of BuChE

On the contrary, Deutetrabenazine had a significantly higher (> 1) number of hydrogen bonds formed. The three complex's free energy analysis also validated our previous analysis of RMSD, Rg and RMSF. Both Donepezil (-125.99 kJ/mol) and Deutetrabenazine (-124.10 kJ/mol) showed lower binding energy as compared to Siponimod (-119.97 kJ/mol) (Table 5.6). The results indicate that Deutetrabenazine binds with the active site residues and other critical residues almost with a similar affinity as the positive control donepezil. Additionally, it was also seen that Siponimod interacts primarily at a different site in the protein as compared to Deutetrabenazine. The overall binding energy also agrees with the binding energy based on our docking results, where there was not much difference between the overall binding energy of these three complexes.

**Table 5.6-** MM/PBSA free energy analysis of Donepezil, Brexipiprazole and Siponimod in complex with acetylcholinesterase, SASA is Surface Accessible Surface Area.

| Ligand | Van Der Waals (kJ/mol) | Electrostatic (kJ/mol) | Polar Solvation (kJ/mol) | SASA (kJ/mol) | Binding Energy (kJ/mol) |
|---|---|---|---|---|---|
| Donepezil | -155.618±12.21 | -4.486±6.51 | 49.813±10.93 | -15.702±1.335 | -125.99±13.37 |
| Deutetrabenazine | -156.936±58.503 | -2.88±5.39 | 50.723±30.91 | -15.008±6.439 | -124.10±41.75 |
| Siponimod | -163.822±12.436 | -0.107±2.979 | 61.609±25.035 | -17.657±1.697 | -119.97±25.37 |

### 5.3.4 ADME analysis results:

We performed a standard ADME analysis of all the four top drug molecules along with Donepezil. All the drug molecules except Siponimod do not violate Lipinski's rule. Deutetrabenazine and Brexipiprazole also follow Lipinksi's rule and can be used for animal and clinical trials studies as potential molecules (Table 5.7).

**Table 5.7-** ADMET analysis of top 5 drugs across both the proteins taken in this study. We analysed the drugs for their drug likeliness and the following Lipinski's rule and its various parameters.

| Molecule | LogP | TPSA (Angstrom)$^2$ | MW (Da) | H-Donor | H Acceptor | Log S | Lipinski |
|---|---|---|---|---|---|---|---|
| Pimavanserin | 4.29 | 44.81 | 427.55 | 1 | 4 | -4.97 | Yes; 0 violation |
| **Deutetrabenazine** | 2.94 | 38.77 | 323.46 | 0 | 4 | -3.63 | Yes; |
| Siponimod | 5.79 | 62.13 | 516.60 | 1 | 8 | 1.23 | No; 2 violations |
| **Brexpiprazole** | 4.41 | 76.81 | 433.57 | 1 | 3 | -5.46 | Yes; 0 violation |
| **Donepezil** | 4 | 38.77 | 379.49 | 0 | 4 | -4.81 | Yes; 0 violation |

## 5.4 Discussion:

This computational work's main aim was to identify specific drugs already approved by the FDA for other neuropsychiatric conditions that could also serve as cholinesterase inhibitors. We performed systematic molecular docking, validated our molecular docking results and performed a molecular simulation to obtain a precise result in both butyrylcholinesterase and acetylcholinesterase. We chose the top two drug molecules and Donepezil based on the molecular analysis, which consistently showed better binding affinity and lowers energy than Rivastigmine and Galanthamine. In the case of acetylcholinesterase, we found that Deutetrabenazine showed better interactions with critical residues, including Tyr336 forming hydrogen bonds. Other critical residues included Pi-alkyl interactions with Tyr340, Phe296, and Phe337. The identical residues also showed possible hydrophobic interactions. It also showed Pi-cation interactions with Tyr285. Deutetrabenazine showed a carbon-hydrogen bond with Asp73. Van Der Waals's interaction around the Oxyanion hole (Phe120 and Tyr123) and CAS (Phe331) and with amino acids of PAS (Asp 73 and Trp285) possibly hints at multiple mechanisms with which the Deutetrabenazine can be an effective acetylcholinesterase inhibitor. Binding to areas around the Oxyanaion hole and CAS indicates the modulation of hydrolysing heavy esters, which are dominantly performed by these

sites. As reported by previous studies, the interaction of potential inhibitors with these residues is critical (Kumar *et al.*, 2017, Zhang *et al.*, 2018).

Most importantly, interaction with PAS residues indicates that it can also affect the central catalytic triad's performance as PAS is directly associated with modulating activities of the main active site. Our simulation results also indicated that Deutetrabenazine could be one of the most critical molecules through multiple analyses, which could be a game-changer as an acetylcholinesterase inhibitor. However, it is essential to carry out proper clinical investigations to validate this hypothesis fully. Siponimod did not show many interactions in our areas of interest. This drug also failed to comply with Lipinski's rules and showed violations in two areas.

On the other hand, based on this study, we can hypothesise that Brexipiprazole and Pimavanserin form strong interactions with key residues of the enzyme compared to Donepezil. Our molecular docking results indicated that both Pimavanserin and Brexipirazole could follow similar mechanisms of inhibition of these enzymes. The drug molecules form a hydrogen bond with residues Gly116 and Gly117, which form the oxyanion hole similar to acetylcholinesterase. Further, these molecules also show interactions with Asp70, which forms the P-site. Interactions of molecules with these residues imply product release blocking and further reducing enzymatic activity. Pimavanserin and Brexipirazole show hydrophobic and Pi-stacking interactions with another critical residue, Tyr332. This residue is known to bind to both the substrate and inhibitor. Interaction of the drugs with these residues implies that they can compete with the substrate and reduce the substrate's access to the active site, further altering the efficiency through any conformational change. These molecules also show strong interactions with active site residues, including Ser198 and His438, thus implying direct inhibitory activity towards the enzyme. Our simulation analysis also indicated that Brexipirazole could be a better candidate than Pimavanserin, showing significantly lower energy than Donepezil and Pimavanserin. The other analyses also showed a better impact of Brexipiprazole on the enzyme, as shown in our RMSD and Radius of gyration results.

## 5.5 Conclusion:

Ageing and various conditions related to ageing, such as dementia, frontotemporal dementia (FTD) and conditions specifically neurodegenerative, have plagued the geriatric population for hundreds of years. Ageing-related mental health problems and neurodegenerative conditions are increasingly common these days, much as a by-product of the increasing life expectancy and increased lifespan. One of the alarming factors in medical science is the mere complexity of these diseases. A reflection of these is seen in the limited number of medications and treatment options the doctors often have to cure them. Patients, after a point in time, often refuse treatment. Drug repurposing is a potential solution given the slow nature of drug discovery for complex diseases such as Alzheimer's, Parkinson's, and other commonly presenting neurodegenerative diseases. The central theme of this paper is solely based on the idea of repurposing a particular approved, investigational drug by the FDA. Based on our results, we suggest Brexipiprazole as a potential butyrylcholinesterase inhibitor and Deutetrabenazine as a potential acetylcholinesterase inhibitor. Although being preliminary analyses, these molecules require further validation through extensive animal-based studies and actual clinical data. Our group is extensively involved in experimental work on essential proteins (Lee *et al.*, 2008; Saudagar *et al.*, 2011).